European Journal of Pharmaceutics and Biopharmaceutics 73 (2009) 260–268

Contents lists available at ScienceDirect

European Journal of Pharmaceutics and Biopharmaceutics

journal homepage: www.elsevier.com/locate/ejpb

Research paper

Relating solubility data of parabens in liquid PEG 400 to the behaviour of PEG 4000-parabens solid dispersions

Johan Unga [a,1], Farhad Tajarobi [a,b], Ove Norder [a], Göran Frenning [c], Anette Larsson [a,*]

[a] Department of Chemical and Biological Engineering, Chalmers University of Technology, Göteborg, Sweden
[b] AstraZeneca R&D, Mölndal, Sweden
[c] Department of Pharmacy, Uppsala University, Uppsala, Sweden

ARTICLE INFO

Article history:
Received 28 April 2008
Accepted in revised form 2 June 2009
Available online 7 June 2009

Keywords:
Solid dispersions
Polyethylene glycol
Solubility
Differential scanning calorimetry
Small angle X-ray diffraction
Wide angle X-ray diffraction

ABSTRACT

The solid state behaviour of polyethylene glycol 4000 (PEG 4000) and dispersions of a homologous series of parabens (methyl- (MP), ethyl- (EP), propyl- (PP) and butyl- (BP)) were examined and compared to the paraben solubility in liquid PEG 400. Dispersions were prepared by co-melting different amounts of paraben (5–80% (w/w)) and PEG 4000 and were studied using a combination of differential scanning calorimetry (DSC) and small and wide angle X-ray diffraction (SAXD/WAXD). Depending on the concentration of parabens in the dispersions, DSC showed melting peaks from folded and unfolded forms of PEG, a eutectic melting and melting of pure parabens. The fraction of folded PEG increased and the melting temperatures of both PEG forms decreased with increasing paraben content. In an apparent phase diagram of PP–PEG dispersions a eutectic mixture appeared above 5% PP. In addition, a melting peak corresponding to the paraben appeared for dispersion containing more than 60% PP. Similar phase diagrams were shown for the other parabens. The SAXD data and a 1D correlation function analysis revealed that MP and BP were incorporated into the amorphous domains of the lamellae of solid PEG to a higher degree than EP and PP. In addition, the lamellae thickness of PEG and the fraction of amorphous domains increased more for MP and BP compared to EP and PP. BP showed the highest solubility of the parabens followed by MP, EP and PP in both liquid and solid PEG. Furthermore, the thickness of the amorphous domains of the PEG in the different parabens–PEG dispersions could be correlated to the solubility in liquid PEG 400.

1. Introduction

The use of solid dispersions is not a novel feature in the formulation of drugs. In 1971, Chiou and Riegelmann published a review on the subject [1] which has been followed by more recent reviews [2,3]. Much interest still remains for solid dispersions and solid solutions, mainly due to the use of these systems to increase the dissolution rate of drug substances [4–9]. The most common methods for preparing solid dispersions are the solvent evaporation [7,10–13] and the fusion methods [9,12], but supercritical fluid methods have also been used [6]. The mechanism of drug release from polymeric solid dispersions has been reviewed by Craig [14]. In such systems, the simplest solid dispersions consist of the drug substance and the carrier material which can result in either dissolution of the substance or dispersion as small domains within the matrix.

The materials commonly used in the solid dispersion technology are sugars [5,12,15], lipids [8,16], urea [13] and polymers such as polyvinyl pyrrolidone [10] and polyethylene glycol (PEG) [7,17]. Depending on the molecular weight, PEGs exist both as clear viscous liquids (Mw 200–600) and as white, waxy solids (Mw > 900) at room temperature. In the preparation of solid dispersions, PEGs of molecular weights ranging from 2000 to 20,000 are often used [4]. In the solid state PEG forms lamellar structures with alternating crystalline and amorphous regions [18,19]. The thicknesses of the lamellae depend primarily on the molecular weight of the polymer and on the thermal history of the system. PEGs up to molecular weights of 6000 g/mol can form extended chain crystals in which the polymer chains are extended to their full length, whereas higher molecular weight PEGs form crystals in which each polymer molecule is folded a certain number of times [19]. However, if crystallized at room temperature polymers with molecular weights above approximately 3000 g/mol commonly form metastable or stable-folded crystals. The number of folds on each polymer molecule at equilibrium depends mainly on the chain length. For PEG 4000 the once-folded form is meta-stable and the unfolded form is the stable one, whereas for PEG 6000 the once-folded is stable. In many cases, if a melt is cooled, crystals of higher folding are

* Corresponding author. Department of Chemical and Biological Engineering, Chalmers University of Technology, Göteborg, Sweden. Tel.: +46 31 772 2763.
E-mail address: anette.larsson@chalmers.se (A. Larsson).
[1] Present address: Department of Physical and Analytical Chemistry, Uppsala University, Uppsala, Sweden.

0939-6411/$ - see front matter © 2009 Elsevier B.V. All rights reserved.
doi:10.1016/j.ejpb.2009.06.003

formed at first (primary crystallization) and over time a secondary crystallization process occurs during which the molecules unfold to take the stable form. During the unfolding process a transition state of non-integrally folded molecules has also been reported to occur [20,21].

Many studies have mainly been concerned with the solid state of the drug substances in solid dispersions, e.g. as in Refs. [15,22]. Lately, studies that also consider the solid state of the carrier material and the effect the addition of a foreign substance has on the carrier have been published, e.g. [7,23]. However, there is still a lack of studies where the solubility of model substances in liquid PEG and their solubility in the amorphous parts of solid PEG have been investigated, and the effects of model substances on the solid state properties of PEG.

In the present study, we have examined solid dispersions of PEG 4000 and a homologous series of four different parabens (alkyl-4-hydroxybenzoates) differing only in the length of the alkyl chain. The aim has been to evaluate the formulations from the perspective of both components, both the added parabens and the polymer carrier. As previously mentioned, additives can be dissolved in the amorphous parts of the PEG structure. Our hypothesis was that the solubility of a substance in liquid PEG would correlate to the behaviour of the substances in the amorphous domains of the PEG solid dispersions. The study was performed using a combination of solubility determinations in liquid PEG, X-ray techniques, both small and wide angle X-ray diffractions and differential scanning calorimetry.

2. Materials and methods

Polyethylene glycol 400 (PEG 400) (molecular weight around 400 g/mol) and polyethylene glycol 4000 (PEG 4000) (average molecular weight 4000 g/mol (range: 3500–4500 g/mol)) were of pharmaceutical grade and purchased from Fluka (Germany). Methyl paraben (MP), Ethyl paraben (EP), Propyl paraben (PP) and Butyl paraben (BP) were all >99% pure and purchased from Sigma–Aldrich (Germany). The paraben structures are depicted in Fig. 1. All chemicals were used without further purification.

2.1. Sample preparation

Samples of 5%, 10%, 15%, 25%, 40%, 60% and 80% (w/w, hereafter just denoted %) of each paraben in PEG 4000 were prepared by co-melting. Accurate amounts were weighed into Eppendorf tubes. The samples were melted at 100 °C and kept there for 20 min during intermittent vortex mixing. All melts were clear solutions indicating that no undissolved material remained. The melts were solidified at controlled ambient temperature (21 °C) for 1 day prior to analysis.

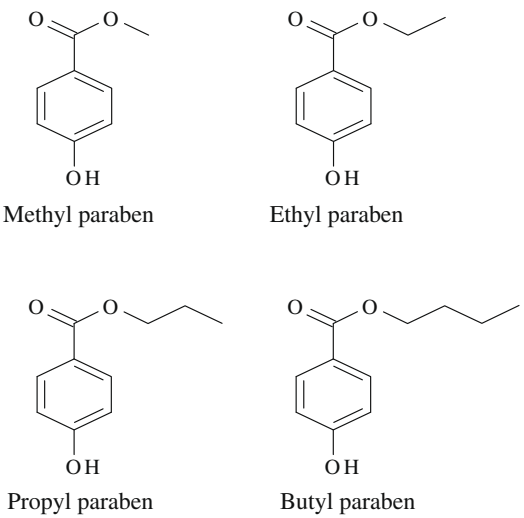

Fig. 1. Molecular structures of the tested parabens.

2.2. Solubility measurements

Saturated solutions were prepared by adding the parabens to liquid PEG 400. This was done by adding incremental amount of parabens to the solution until undissolved paraben was present after 8 h of stirring on a magnetic stirrer. The solutions were stored in a desiccator under dry conditions for a week, after which they were centrifuged and the saturated supernatants were diluted with water below the solubility limit of the parabens in water [24]. The concentrations of the parabens were determined spectroscopically with a Perkin Elmer Lambda 14 UV/Vis Spectrophotometer (Massachusetts, USA) at λ = 255 nm.

2.3. Differential scanning calorimetry

The DSC analysis was performed with a Perkin Elmer DSC 7 equipped with an Intracooler 1P add-on. Calibration of temperature and enthalpy of fusion were performed using indium (temperature of fusion 156.60 °C and enthalpy of fusion 28.51 Jg^{-1}) and zinc (419.53 °C) in a standardized two-point method. Samples were weighed into 25 μl aluminium pans, heated to 140 °C and cooled to 0 °C and again at 10 °C/min, and then stored until analysed. This procedure was used to obtain better contact between the sample and the pan; thus, improving the quality of the thermograms. DSC measurements were performed using two different heating programs accordingly: (i) 0–70 °C (5 °C/min), 70–140 °C (40 °C/min), 140–0 °C (5 °C/min) and (ii) 0–140 °C (40 °C/min). The low scanning speed up to 70 °C according to heating program (i) was chosen to get good resolution for the PEG melting and the fast, thereafter, to be able to detect melting of pure paraben before it dissolved in the melted PEG. The second temperature program was used to improve the possibilities to investigate the melting of the parabens in the dispersions. Pure PEG 4000 was examined in the same manner as the dispersions. All DSC measurements were performed in duplicates.

2.4. Wide angle X-ray diffraction

Wide angle X-ray diffraction measurements were performed on the 5–25% samples on a Kratky camera (Hecus X-ray Systems, Graz, Austria) with CuK_α radiation of λ = 0.1542 nm provided by a Philips PW 1830/40 generator operated at 50 kV and 40 mA. A tungsten beam stop was used. Data were recorded during 15 min for each sample under vacuum.

2.5. Small angle X-ray measurements

Small angle X-ray diffraction measurements were performed on the 5%, 15%, 25% and 40% samples at beamline I711 at Max-lab (Lund university, Lund, Sweden) [25]. The radiation wavelength was 0.1125 nm. Diffractograms were recorded under vacuum at room temperature (20 °C) using a marccd 165 2D detector. The exposure time was 600 s for each sample. The resulting CCD images were integrated using Fit2D software provided by Hammersley [26]. Calibration was performed using tristearin which has a lamellar structure with repeating distances of 0.45 nm.

The repeating distances in the lamellar structures were calculated from the position of the first peak in Lorenz corrected SAXD data using Bragg's law:

$$n\lambda = 2d\sin\theta \quad (1)$$

where n is an integer (1 for the first peak), λ is the X-ray wavelength, d is the distance between repeating planes and θ is one half of the scattering angle.

2.6. SAXD data analysis

The SAXD data were analysed by using the one-dimensional (1D) correlation function $\gamma(x)$, which for a point-collimated X-ray beam is calculated as [27]:

$$\gamma(x) = \frac{\int_0^\infty q^2[I(q) - I_b]\cos(xq)dq}{\int_0^\infty q^2[I(q) - I_b]dq} \quad (2)$$

where $I(q)$ is the experimental intensity, I_b is a background (assumed to be independent of q in the region of interest) and $q = (4\pi/\lambda)\sin\theta$ is the magnitude of the scattering vector (with 2θ being the scattering angle and λ the wavelength, as before). In order to calculate the integrals in Eq. (2), the experimental data were extrapolated to infinite q by using the Porod–Ruland model [28]:

$$I(q) = K\frac{\exp(-\sigma^2 q^2)}{q^4} + I_b \quad (3)$$

and to zero q by using the Debye–Bueche model [29,30]:

$$I(q) - I_b = \frac{I_0}{(1+\xi^2 q^2)^2}. \quad (4)$$

In these expressions, K, σ, I_0 and ξ are constants. First, I_b, K and σ were determined by fitting Eq. (3) to the intensity at high q (typically $\geqslant 2\ \mathrm{nm}^{-1}$); thereafter, I_0 and ξ were determined by fitting Eq. (4) to the background-corrected intensity at low q. The latter fit was typically done for $q \leqslant 0.2\ \mathrm{nm}^{-1}$. Sometimes the primary beam was found to adversely affect the calculated 1D correlation function, and in those cases a few of the data points at low q were disregarded.

3. Results and discussion

3.1. Solubility measurements

The solubility of the different parabens in liquid PEG 400 was highest for BP (397 g/L, 2.04 mol/L) followed by MP (272 g/L, 1.79 mol/L), EP (241 g/L, 1.45 mol/L) and PP (224 g/L, 1.24 mol/L). The similarity in solubility of MP and BP in PEG 400 is somewhat surprising since MP is the most hydrophilic and BP is the least hydrophilic of the parabens. This implies that the hydrophilicity is not the decisive factor for deciding the solubility of the parabens in PEG as it is in water. This behaviour can be explained by more favourable interactions between PEG and MP/BP compared to PEG and EP/PP.

3.2. Differential scanning calorimetry

All parabens affected the melting and crystallization of PEG in a concentration dependent manner. Fig. 2a displays the thermograms from heating of the pure PEG, PP–PEG dispersions and pure PP according to the heating program (ii) (40 °C/min). Samples containing only PEG showed one melting peak in the applied heating program. Moreover, as the PP content in the dispersions increased up to 25% a shoulder at lower temperatures appeared and the

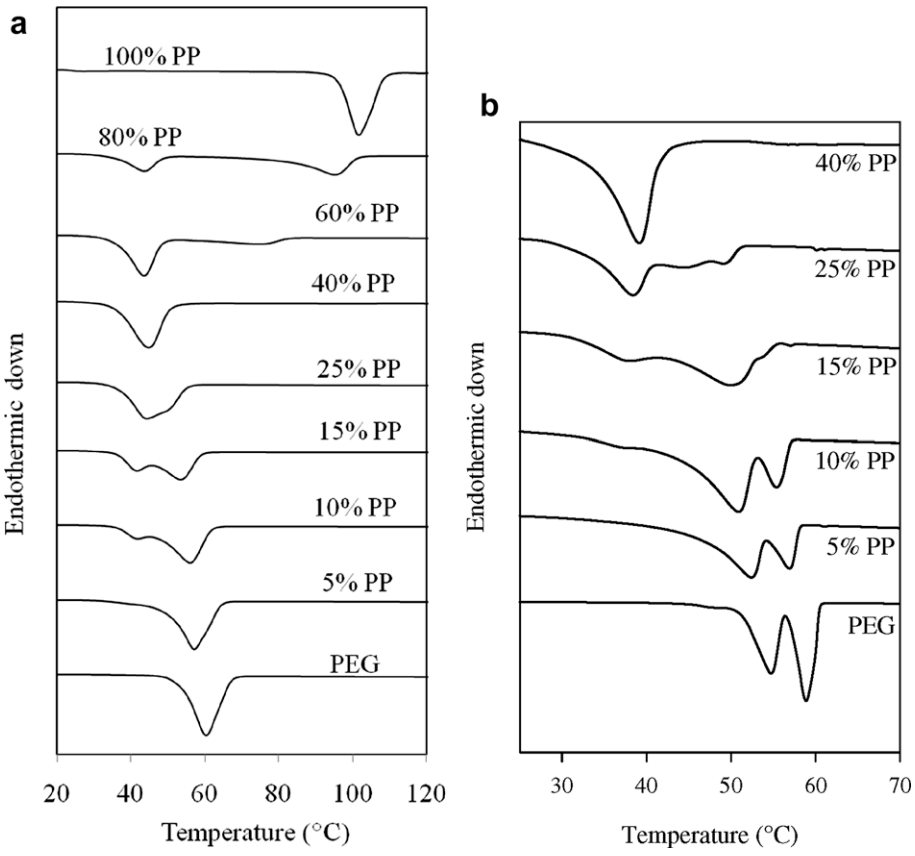

Fig. 2. (a) Thermograms from heating of samples stored 1 day in PEG 4000 (bottom) with increasing concentration (5%, 10%, 15%, 25%, 40%, 60%, 80% PP and pure PP). Scanning rate 40 °C/min. (b)Thermograms from heating of samples stored 1 day in PEG 4000 (bottom) with increasing concentration (5%, 10%, 15%, 25% and 40%) of PP. The heat flow has been weighted to the amounts of PEG in each sample. The scanning rate was 5 °C/min.

melting temperature for the original peak decreased. The peak with low melting temperature appeared at approximately the same melting temperature in all concentrations. Further, a gradual decrease in size of the original peak and an increase in size of the other peak occured with increasing paraben content for the dispersions containing below 25% PP. At 40% PP only a single peak is visible. For the dispersions with PP concentration of 80% a new peak at higher temperature (around 90 °C, Table 1) emerges, and a closer inspection of the thermogram for 60% PP also shows an indication of a second melting peak at around 75–80 °C. For pure PP melting was observed at about 100 °C.

As seen in Fig. 2b, using a slower scanning rate (method i with 5 °C/min in scanning rate) provided a better resolution for detecting different forms of PEG in the dispersions than a faster scanning rate was used (method ii; Fig. 2a). For pure PEG two melting peaks at 54 and 58 °C, respectively, for PEG appeared using method i. These peaks are found in the literature corresponding to folded and unfolded PEG chains, respectively [18]. At low concentrations (0–5%) only the folded and unfolded forms of PEG could be detected. From dispersions containing 10% PP a third peak appeared which grew with increasing PP content. Ultimately, at 40% PP concentration, this peak was the only one detected in the thermogram. At intermediate concentrations of PP (15–25%) there was a system containing folded PEG, unfolded PEG which is presumably a eutectic mixture exhibiting a melting point at approximately 38 °C. At 60% and 80%, PP the eutectic peak decreased and a new peak above the melting point of pure PEG appeared (Table 1 and 2).

Fig. 3 displays how the melting temperatures of the solid dispersions vary with increasing amount of parabens. As seen in Fig. 2b, up to three different peaks appeared in the same thermogram. Fig. 3 is an apparent phase diagram and strictly not equivalent to a true phase diagram, since a phase diagram can only be made for systems in equilibrium. However, samples stored only 1 day are not in equilibrium, since transformation from folded to unfolded PEG forms occurs during months [31]. The apparent phase diagrams show for all investigated parabens that the melting temperatures of the unfolded and the folded PEG decreases with increasing paraben concentration until a certain point is reached, after which the melting temperature for parabens increased with increasing paraben concentration. At the same time, the melting temperature for the eutectic mixture is more or less constant. Taken together, this supports the picture of a eutectic system.

The overall conclusion is that the melting behaviours of the all investigated parabens–PEG dispersions resemble each other (Table 1 and 2, and Fig. 3), which indicate large similarities between the dispersions. The most obvious difference between the dispersions is that the eutectic melting temperature for BP dispersions is lower than those for the other paraben dispersions (Table 1). Another difference is that the eutectic peak appears at larger fractions of parabens for MP and BP than for EP and PP. Also seen in the Fig. 3 is that the slopes for the melting temperatures of folded and unfolded PEG were similar for all paraben dispersions, but there is a small tendency that the melting slopes for BP are somewhat less steep,

Table 1
Melting temperatures for folded and unfolded PEG, eutectic mixtures and parabens[a,b,c,d].

	Amount paraben	T_m (folded) (°C)	T_m (unfolded) (°C)	T_m (eutectic) (°C)	T_m (paraben) (°C)
PEG	4000	0	54.1 ± 0.4	58.1 ± 0.6	n.p.
n.p.					
MP	0.05	51.2 ± 0.2	55.8 ± 0.1	n.p.	n.p.
MP	0.1	51.0 ± 1.1	55.6 ± 0.6	n.p.	n.p.
MP	0.15	44.8 ± 0.1	51.7 ± 0.1	n.p.	n.p.
MP	0.25	n.p.	n.p.	33.8 ± 1.2	n.p.
MP	0.40	n.p.	n.p.	33.2 ± 0.1	n.p.
MP	0.60	n.p.	n.p.	33.9 ± 2.0	91.6 ± 8.8
MP	0.80	n.p.	n.p.	31.5 ± 2.0	109.1 ± 1.7
MP	1.00	n.p.	n.p.	n.p.	131.1 ± 0.3
EP	0.05	51.8 ± 0.4	56.0 ± 0.5	n.p	n.p.
EP	0.1	49.5 ± 0.8	54.1 ± 0.7	36.0 ± 0.2	n.p.
EP	0.15	47.3 ± 0.2	51.2 ± 0.8	38.6 ± 0.4	n.p.
EP	0.25	n.p.	n.p.	40.0 ± 0.1	n.p.
EP	0.40	n.p.	n.p.	39.9 ± 0.1	n.p.
EP	0.60	n.p.	n.p.	40.6 ± 0.3	93.2 ± 0.3
EP	0.80	n.p.	n.p.	40.0 ± 0.1	113.1 ± 0.3
EP	1.00	n.p.	n.p.	n.p.	121.5 ± 0.2
PP	0.05	52.1 ± 0.4	56.3 ± 0.6	n.p.	n.p.
PP	0.1	50.5 ± 0.6	54.6 ± 0.9	37.1 ± 0.1	n.p.
PP	0.15	49.5 ± 0.5	53.0 ± 0.8	37.5 ± 0.3	n.p.
PP	0.25	44.0 ± 0.4	48.4 ± 0.8	38.3 ± 0.2	n.p.
PP	0.40	n.p.	n.p.	39.0 ± 0.2	n.p.
PP	0.60	n.p.	n.p.	38.4 ± 0.2	76.2 ± 0.8
PP	0.80	n.p.	n.p.	37.3 ± 0.2	95.4 ± 0.1
PP	1.00	n.p.	n.p.	n.p.	101.5 ± 0.0
BP	0.05	51.9 ± 0.5	56.5 ± 1.0	n.p.	n.p.
BP	0.1	50.6 ± 0.9	55.1 ± 1.1	n.p.	n.p.
BP	0.15	48.0 ± 0.2	52.6 ± 0.1	n.p.	n.p.
BP	0.25	44.4 ± 0.2	n.p.	30.1 ± 0.4	n.p.
BP	0.40	n.p.	n.p.	30.1 ± 0.5	n.p.
BP	0.60	n.p.	n.p.	30.2 ± 0.4	n.p.
BP	0.80	n.p.	n.p.	30.9 ± 1.9	64.1 ± 0.1
BP	1.00	n.p.	n.p.	n.p.	72.7 ± 0.1

[a] n.p. Means that no peak was observed in the thermogram.
[b] ± Number means the half error between two measurements.
[c] Scanning rate was 5 °C/min.
[d] The presented data are average of two measurements and ± the half difference between the measurements are given in table.

Table 2
Melting enthalpies folded and unfolded PEG, eutectic mixtures and the total enthalpies[a,b,c,d].

	Amount paraben	ΔH_m(folded) (J/g)	ΔH_m (unfold) (J/g)	ΔH_m (eutectic) (J/g)	$\Delta H_{m,tot}$ (J/g)
PEG	4000	0	89 ± 3	86 ± 1	n.p.
	174 ± 2				
MP	0.05	117 ± 2	48 ± 2	n.p.	166 ± 1
MP	0.1	86 ± 6	43 ± 6	n.p.	138 ± 5
MP	0.15	93 ± 1	32 ± 1	n.p	125 ± 1
MP	0.25	n.p.	n.p.	124 ± 3	124 ± 3
MP	0.40	n.p.	n.p.	117 ± 3	119 ± 2
MP	0.60	n.p.	n.p.	60 ± 11	142 ± 11
MP	0.80	n.p.	n.p.	27 ± 13	138 ± 4
MP	1.00	n.p.	n.p.	n.p.	168 ± 2
EP	0.05	108 ± 2	65 ± 8	n.p.	172 ± 9
EP	0.1	99 ± 4	35 ± 4	28 ± 1	162 ± 6
EP	0.15	69 ± 1	29 ± 1	58 ± 1	156 ± 2
EP	0.25	n.p.	n.p	111 ± 4	146 ± 1
EP	0.40	n.p.	n.p	118 ± 1	118 ± 1
EP	0.60	n.p.	n.p.	108 ± 19	141 ± 22
EP	0.80	n.p.	n.p.	50 ± 1	163 ± 1
EP	1.00	n.p.	n.p.	n.p	155 ± 1
PP	0.05	110 ± 1	36 ± 2	n.p.	147 ± 2
PP	0.1	85 ± 8	28 ± 2	13 ± 3	141 ± 3
PP	0.15	85 ± 1	21 ± 5	48 ± 1	161 ± 1
PP	0.25	36 ± 2	12 ± 1	96 ± 2	143 ± 3
PP	0.40	n.p.	n.p.	124 ± 2	124 ± 2
PP	0.60	n.p.	n.p.	87 ± 1	116 ± 1
PP	0.80	n.p.	n.p.	34 ± 1	109 ± 1
PP	1.00	n.p.	n.p.	n.p.	154 ± 1
BP	0.05	114 ± 3	36 ± 1	n.p.	150 ± 3
BP	0.1	103 ± 5	32 ± 3	n.p.	135 ± 2
BP	0.15	82 ± 13	31 ± 1	n.p.	141 ± 5
BP	0.25	86 ± 3	n.p.	50 ± 5	137 ± 6
BP	0.40	n.p.	n.p.	120 ± 2	120 ± 2
BP	0.60	n.p.	n.p.	113 ± 4	113 ± 4
BP	0.80	n.p.	n.p.	39 ± 3	113 ± 5
BP	1.00	n.p.	n.p.	n.p.	133 ± 1

[a] n.p. Means that no peak was observed in the thermogram.
[b] ± Number means the half error between two measurements.
[c] The scanning rate was 5 °C/min.
[d] The presented data are average of two measurements and ± the half difference between the measurements are given in table.

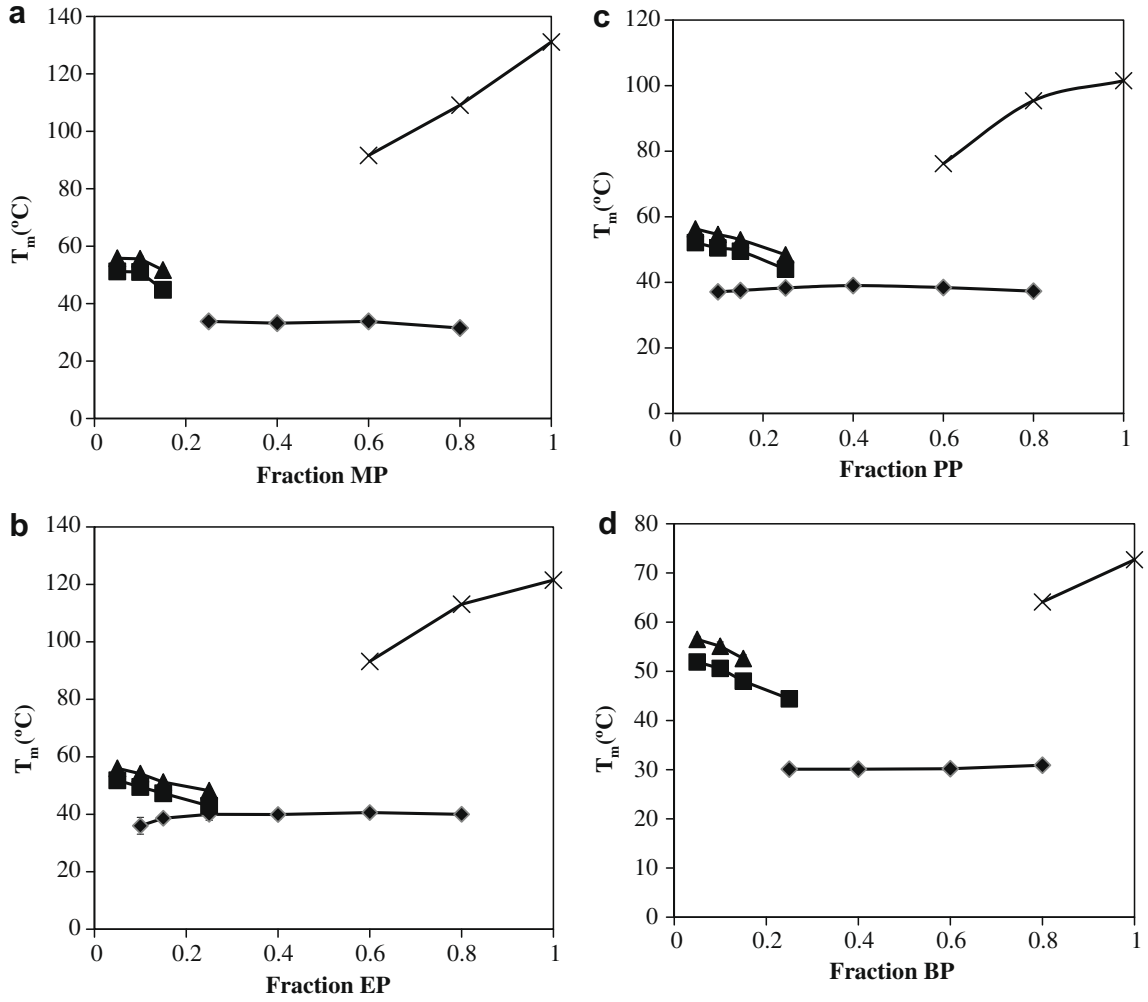

Fig. 3. Melting temperatures for the unfolded (▲), folded form (■) of PEG, the eutectic mixture (♦) and (×) pure parabens for (a) MP, (b) EP, (c) PP and (d) BP. Presented data are average of two replicates. The standard errors are presented in Table 1. The scanning rate was 5 °C/min.

followed by the other ones. The slope relates to the content in the eutectic point, where the lower slope for BP indicates that BP has a higher content of the paraben in the eutectic point compared to the other ones.

Fig. 4 displays the enthalpies for the melting peaks and the total melting enthalpy for the different concentrations of the parabens. The behaviour for the parabens resembles each other. To calculate the enthalpies for the unfolded and folded peaks a line in the local minima between the peaks was drawn, and the peak areas left and right of this line were assumed to correspond to the folded and the unfolded forms, respectively.

For pure PEG the enthalpy for folded form was approximately equal to that of the unfolded form. Upon addition of the parabens, the total melting enthalpies for unfolded and folded PEG decreased with increased parabens concentration. Also, the ratio between the enthalpy for folded and the unfolded PEG increased with paraben addition, which indicates that parabens promote the folding of PEG.

The enthalpy for melting the eutectic mixture reaches a maximum at about 40% PP (Fig. 4). This means that the fraction of eutectic mixture is the largest at this point. At this composition, the melting enthalpy of the eutectic mixture is equal to the measured total enthalpy, since no other peaks could be detected. The total enthalpy was lower or equal for pure PEG compared to the total enthalpy for any of the dispersions. This indicates that even a small addition of 5% paraben increases the degree of crystallinity of PEG. The total enthalpy is the sum of the enthalpies for melting of the unfolded and folded PEG, as well as the melting of the eutectic mixture and the parabens. In addition to this, dissolution of the parabens in the PEG melt can occur. This dissolution process will of course also be an enthalpic process, but it will not appear as a distinct peak in the DSC thermograms and might, therefore, not be fully accounted for.

3.3. Wide angle X-ray diffraction

Wide angle X-ray diffraction was used to assess the presence of crystalline drug in the dispersions. Diffractograms from measurements on the pure parabens show distinct peaks, which is evidence of a crystalline structure and exemplified as for PP and BP in Fig. 5. Pure PEG shows two rather broad peaks around 19.2° and 23.3° corresponding to repeating distances of 0.46 nm and 0.38 nm, respectively. To assess the sensitivity of the method physical mixtures of 2% and 5% of the parabens and PEG 4000 were used (data not shown). The 2% of samples did not display any peaks from the crystalline parabens, but the 5% paraben samples did, which shows that the sensitivity for detecting crystalline parabens with this method is between 2 and 5%.

The diffractograms from the 25% paraben samples all showed peaks corresponding to peaks in the diffractograms from the pure

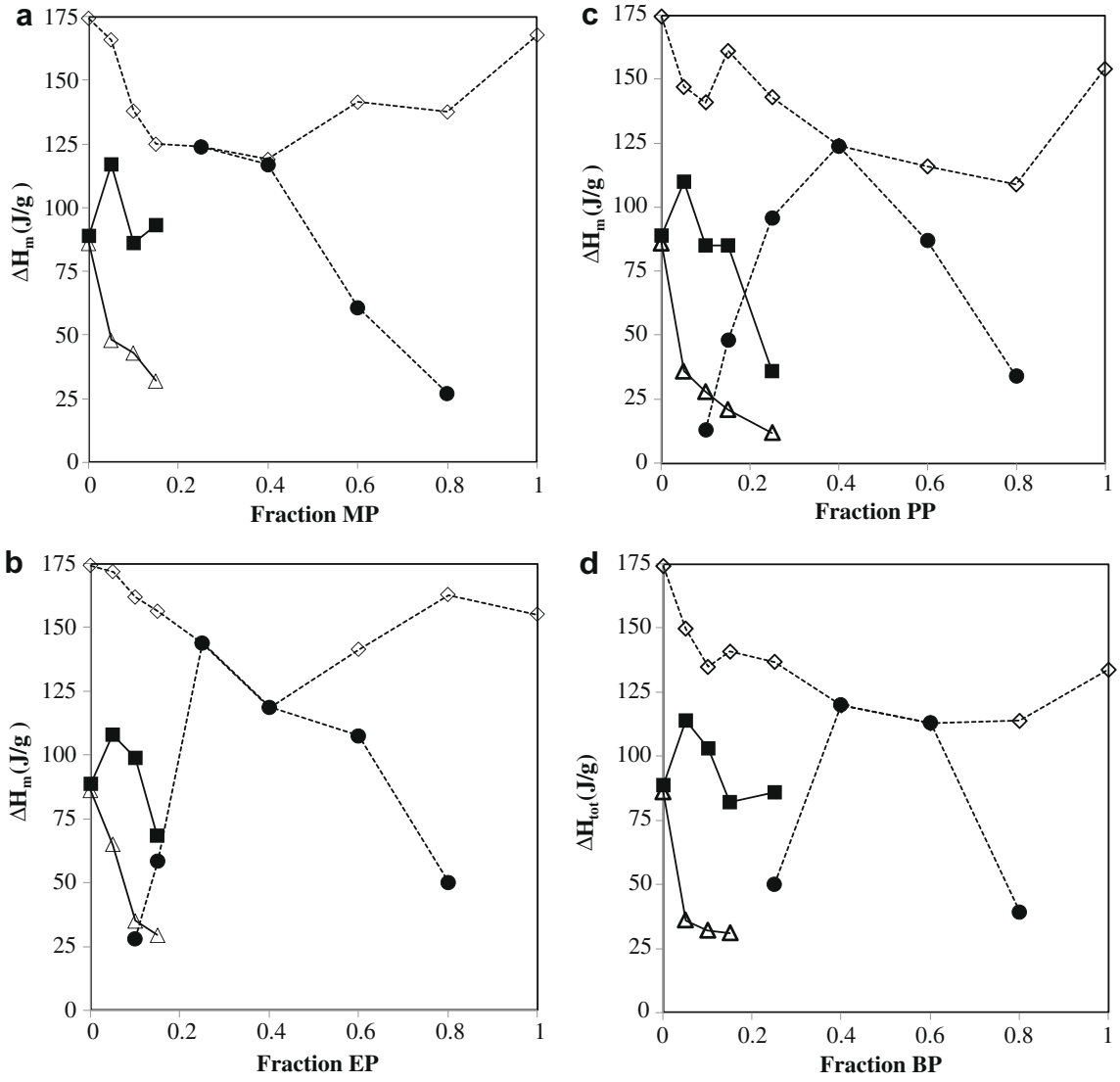

Fig. 4. Melting enthalpies for the parabens dispersions samples after 1 day storage. The different series are the folded PEG (■), unfolded PEG (Δ), the 'eutectic mixture' (●), and the total melting enthalpy (◇) for (a) MP, (b) EP, (c) PP and (d) BP. Presented data are average of two replicates. The standard errors are presented in Table 1. The scanning rate was 5 °C/min.

parabens indicating that crystalline substance was present. In the EP and PP samples, paraben peaks could be detected in the 10% samples, but not in the 5% ones. The peak pattern for PP at concentrations above 10% PP was not exactly the same as for crystalline PP, but it indicates that regular structure is appearing. It may indicate that there is some paraben dissolved in the PEG carrier, but less than 10% (see Fig. 5 for the PP solid dispersions). However, for both MP and BP (BP displayed in Fig. 6), crystalline substance was not seen up to and including the 15% sample, but paraben peaks did appear in the 25% samples demonstrating a higher but still limited solubility of MP and BP in the solid PEG. This higher solubility is in line with the higher solubility for these substances in liquid PEG 400, but to elucidate the questions where in the PEG structure the parabens are dissolved further investigations are needed.

The DSC experiments did not display melting peaks for parabens below 60%, whereas WAXD suggests that there is crystalline paraben at lower concentrations. This is most likely explained by dissolution of paraben in molten PEG during the DSC experiment. This is supported by the high solubilities of the parabens in PEG 400.

3.4. Small angle X-ray measurements

All PEG–paraben samples showed diffraction patterns consistent with lamellar symmetries as would be expected for PEG 4000. Depending on the added paraben the patterns differ (see examples in Fig. 7), the lamellae thicknesses vary and in some samples two different lamellar structures could be seen. In the pure PEG sample only one set of diffraction peaks were visible, the first at $q = 0.46\ \mathrm{nm}^{-1}$ corresponding to a lamellae thickness, d, of 13.7 nm (Table 3), which is roughly what would be expected for the once-folded PEG 4000 [19,21]. From the DSC measurements, it is obvious that also the unfolded form is present, but it does not diffract X-rays to a detectable extent because of having too small electron density difference between crystalline and amorphous domains [30]. Addition of the different parabens affected this behaviour in different ways. No appreciable changes in lamellar thicknesses were seen in the samples with 5% of the parabens compared to the pure PEG, which shows that such a small amounts were not sufficient to affect the PEG structure in such a way that it could be detected with SAXD. However, the diffraction was stronger with the parabens present indicating a larger electron density

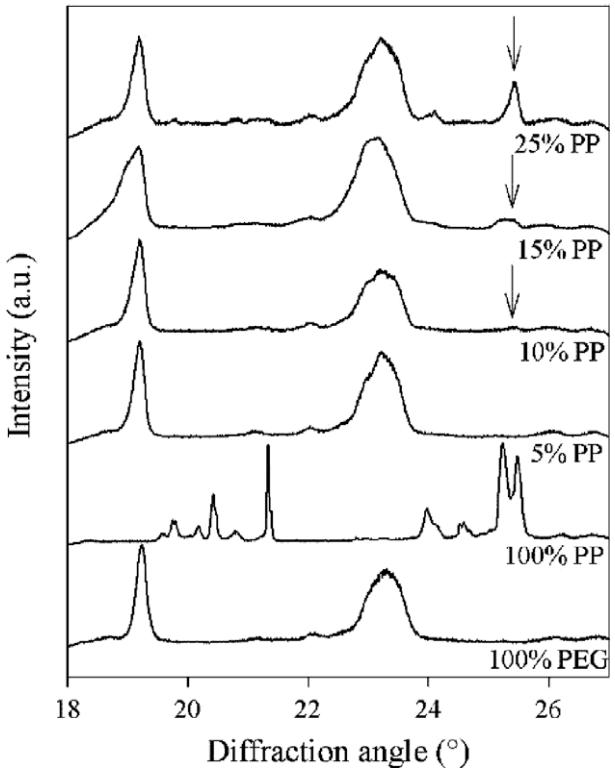

Fig. 5. WAXD diffractograms of pure PEG (bottom), pure PP and solid dispersions with increasing concentration of PP in PEG (5%, 10%, 15% and 25%).

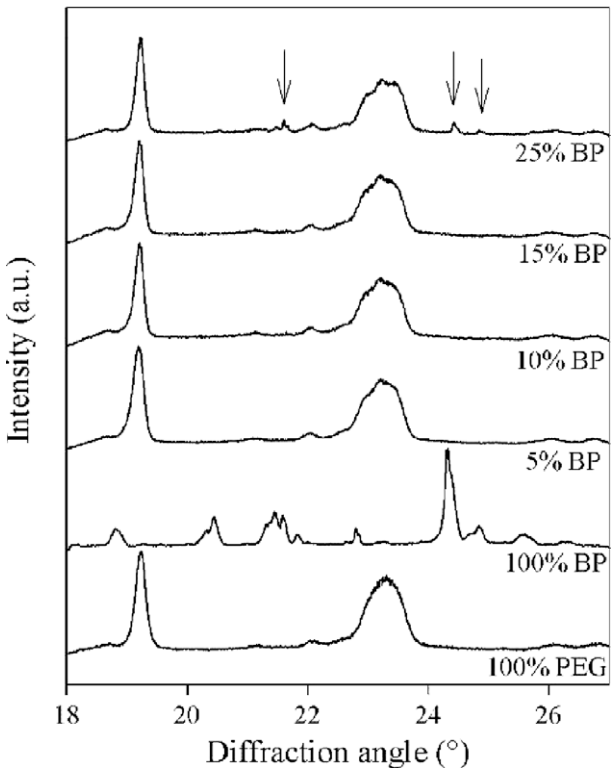

Fig. 6. WAXD diffractograms of pure PEG (bottom), pure BP and solid dispersions with increasing concentration of BP in PEG (5, 10, 15 and 25%). No indication of crystalline BP is seen in the 5–15% samples, but at 25% BP peaks appear.

difference caused by incorporation of paraben in the amorphous domains. At higher concentrations of the parabens the differences between the samples were apparent. For MP 15% and 25% two different sets of peaks showed in the diffractograms, one consistent with the unfolded PEG with d about 26.5 nm, and one around 18 nm. The uncertainties in the SAXD measurements were found to have a standard deviation well below 1 nm, which strongly indicates that the measured thickness of the folded PEG chains is larger in the solid dispersion than for pure PEG. The increased thickness may be due to MP being incorporated in the amorphous domains and forcing a swelling of the structure. In contrast to pure PEG samples, an unfolded lamellar PEG structure for MP–PEG was observed. This fact is an evidence of an increased electron difference indicating that some paraben was incorporated in the PEG structure and thus induced increase in the amorphous domain thickness. The 40% MP sample displayed only one set of peaks (d = 14.3 nm) after 1 day. Taken together, MP seems to increase the lamellar structure thickness.

For EP only diffraction from the folded form with d about 15 nm was seen for all dispersion compositions (15% d = 14.0 nm, 25%

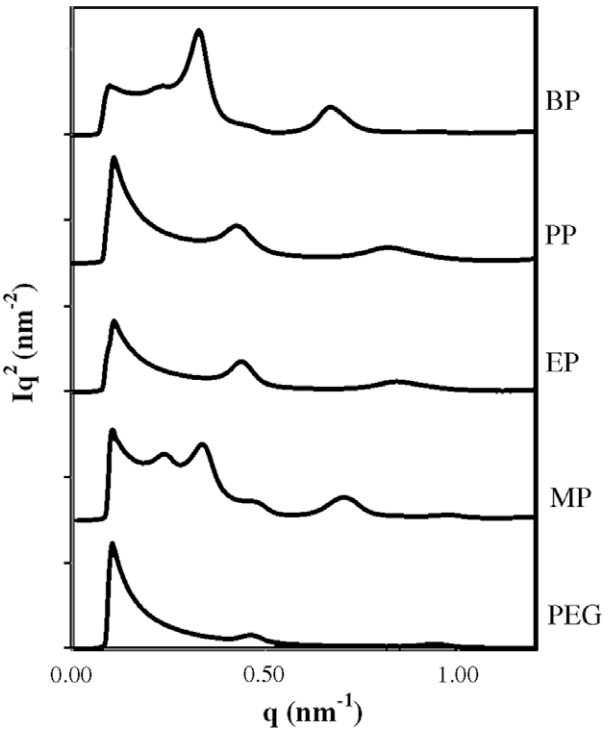

Fig. 7. SAXD diffractograms of samples of 25% of the different parabens in PEG and pure PEG after 1 day storage. From bottom to top: Pure PEG, MP, EP, PP and BP. Pure PEG shows diffraction from one lamellar thickness at q = 0.46 nm^{-1} and 0.92 nm^{-1}. In the EP and PP samples, only one set of peaks is seen, the first peak at q = 0.43 nm^{-1} and q = 0.41 nm^{-1}, respectively. In the MP and BP samples, there are two sets of peaks, the first for MP at q = 0.24 nm^{-1} and q = 0.34 nm^{-1} and for BP at q = 0.22 nm^{-1} and q = 0.35 nm^{-1}.

Table 3
Lamellae thickness, *ds*, and crystalline and amorphous fractions for pure PEG and 25% parabens samples[a,b].

	Folded (nm)	Unfolded (nm)	f_c	f_a
PEG 4000	13.6 ± 0.05	n.d.	0.85	0.15
25% MP	18.5 ± 0.5	26.5 ± 0.5	0.74	0.26
25% EP	14.7 ± 0.6	n.d.	0.82	0.18
25% PP	15.2 ± 0.6	n.d.	0.81	0.19
25% BP	18.1 ± 0.9	28.0 ± 0.7	0.71	0.29

[a] n.d. – No peak was detected.
[b] ±s.d., with n = 3.

d = 15.1 nm, 40% d = 14.1 nm). The diffractograms of the all PP samples showed the presence of the folded form after 1 day and the 40% sample also showed diffraction from unfolded PEG (15% d = 14.5 nm, 25% d = 15.6 nm, 40% d = 15.8 nm, 23.7 nm). Compared to EP the thicknesses are somewhat greater indicative of more paraben being incorporated in the structure. The BP samples containing at least 15% of BP differed from the other paraben samples by displaying two sets of diffraction peaks from PEG, one from a swollen folded form and one from unfolded PEG. BP caused the most swelling of the folded form (15% d = 17.8 nm, 25% d = 19.0 nm, 40% d = 18.7 nm).

3.5. 1D correlation function analysis

The 1D correlation function plots were used to determine the lamellar thicknesses and the degree of crystallinity of the PEG structure, i.e. the crystalline (f_c) and amorphous (f_a) volume fractions, respectively. The total thicknesses (L_{tot}) were in good agreement with those determined directly from the SAXD diffractograms. The lamellae thicknesses and the crystalline and amorphous fractions for pure PEG 4000 and 25% paraben–PEG samples are given in Table 3. As can be seen in the table all parabens increased the amorphous fraction of the PEG. BP (f_a = 0.29) increased it the most followed by MP (f_a = 0.26), which is almost double that of pure PEG (f_a = 0.15).

In Fig. 8 the lamellar thicknesses for all 25% paraben samples and pure PEG are plotted against the fraction of amorphous domain in the structure. It shows that d increases linearly with increasing amount of amorphous material, which supports the notion that the structure consists of once-folded PEG with swollen amorphous domains. The thickness of the crystalline parts was also somewhat larger in the MP and BP samples, but the major part of the increase in lamellae thickness was due to swelling of the amorphous region. MP and BP are also the parabens that have the highest solubility in both liquid and solid PEG.

3.6. Incorporation in liquid vs. solid PEG

Fig. 9 shows the paraben solubilities in liquid PEG 400, and the thickness of the amorphous domains within the PEG 4000 lamellae. The plot gives a hint that a higher solubility in the liquid PEG is connected to the amorphous domains being thicker and thus have larger total volume. This indicates that the parabens with a higher solubility in liquid PEG induces an increased amorphous volume and at the same time is incorporated into that volume. The parabens that have the highest solubility in the liquid PEG 400 also have a high solubility in the amorphous domains of solid PEG 4000.

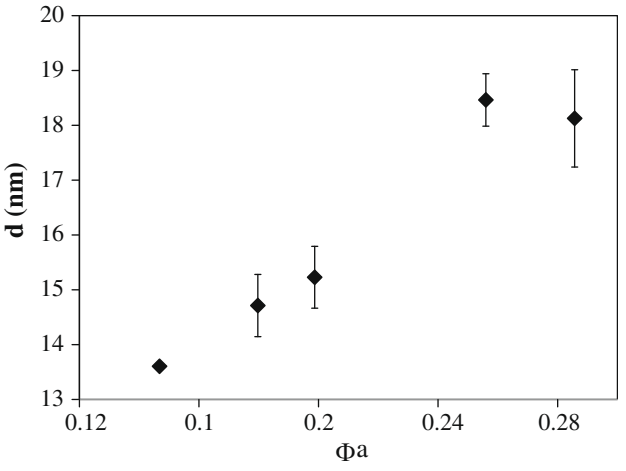

Fig. 8. The lamellar thicknesses (d) plotted against the fraction of amorphous domain (Φ_a) after 1 day for the pure PEG sample and the four 25% paraben samples (n = 3, ±s.d.).

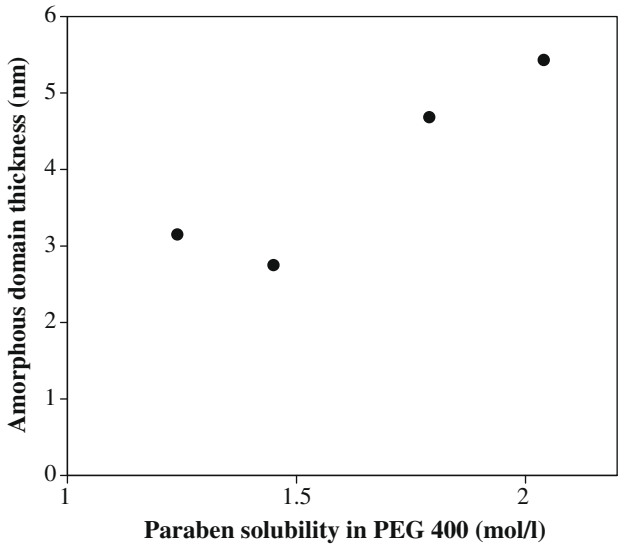

Fig. 9. The thickness of the amorphous domains of the 25% samples and the paraben solubility in liquid PEG 400.

4. Conclusions

The solubility of the parabens in liquid PEG 400 is not primarily depending on the hydrophilicity of the molecules. The most hydrophilic and the least hydrophilic (MP and BP) had the highest solubility in PEG 400 and the two parabens of intermediate hydrophilicity (EP and PP) had lower solubilities. The reason for this is not altogether clear, but MP and BP apparently interact more favourably with PEG. It has been reported that strong interaction between drug and polymer carrier favours formation of amorphous drug in solid dispersions [32]. That explains why the parabens with the highest solubilities are also the ones which stay in a non-crystalline state at higher concentrations in the solid dispersions.

From the DSC analysis apparent phase diagrams could be drawn for the PEG:paraben dispersions. These indicate that eutectic mixture being formed and that the eutectic point occurs at paraben concentrations around 40%. The SAXD studies show that incorporation of MP and BP in PEG made the unfolded PEG peak visible in the diffractograms, which was not the case for pure PEG and dispersions of EP:PEG and PP:PEG. That indicates that MP and BP were dissolved in the amorphous domains between the extended PEG chains, changed the electron density contrast and allowed detection by SAXD. The fact that MP and BP increased the lamellar thickness and induces greater amorphous volumes in the PEG further supports the notion that the parabens are incorporated into the amorphous domains of the PEG as has previously been suggested for a lipid incorporated in PEG [31].

Incorporation of a substance into the liquid-like amorphous domains of PEG 4000 appears to be related to the solubility of the substance in liquid PEG 400. The solubility of the substance in PEG 400 can, therefore, be used to get an indication to how the substance will behave in a solid dispersion with PEG as the carrier material. The experimental determination of solubility of drugs in PEG 400 is a simple method and could serve as a good first step in predicting the behaviour of drug–PEG solid dispersions.

Acknowledgments

The authors would like to thank Yngve Cerenius, Matti Knaapila and Tomas Plivelic at Max-lab for much needed support with the SAXD measurements. Further, The Chalmers Foundation (JU, AL) and the Swedish Research Council (AL, GF) are acknowledged for financial support.

References

[1] W.L. Chiou, S. Riegelmann, Pharmaceutical applications of solid dispersion systems, Journal of Pharmaceutical Sciences 60 (9) (1971) 1281–1302.
[2] A.T.M. Serajuddin, Solid dispersion of poorly water-soluble drugs: early promises, subsequent problems, and recent breakthroughs, Journal of Pharmaceutical Sciences 88 (10) (1999) 1058–1066.
[3] C. Leuner, J. Dressman, Improving drug solubility for oral delivery using solid dispersions, European Journal of Pharmaceutics and Biopharmaceutics 50 (1) (2000) 47–60.
[4] W.L. Chiou, S. Riegelma, Increased dissolution rates of water-insoluble cardiac glycosides and steroids via solid dispersions in polyethylene glycol 6000, Journal of Pharmaceutical Sciences 60 (10) (1971) 1569.
[5] L.V. Allen, V.A. Yanchick, D.D. Maness, Dissolution rates of corticosteroids utilizing sugar glass dispersions, Journal of Pharmaceutical Sciences 66 (4) (1977) 494–497.
[6] S. Sethia, E. Squillante, Solid dispersion of carbamazepine in PVPK30 by conventional solvent evaporation and supercritical methods, International Journal of Pharmaceutics 272 (1–2) (2004) 1–10.
[7] I. Weuts et al., Study of the physicochemical properties and stability of solid dispersions of loperamide and PEG6000 prepared by spray drying, European Journal of Pharmaceutics and Biopharmaceutics 59 (1) (2005) 119–126.
[8] S. Prabhu, M. Ortega, C. Ma, Novel lipid-based formulations enhancing the in vitro dissolution and permeability characteristics of a poorly water-soluble model drug, piroxicam, International Journal of Pharmaceutics 301 (1–2) (2005) 209–216.
[9] N. Ahuja, O.P. Katare, B. Singh, Studies on dissolution enhancement and mathematical modeling of drug release of a poorly water-soluble drug using water-soluble carriers, European Journal of Pharmaceutics and Biopharmaceutics 65 (1) (2007) 26–38.
[10] V. Tantishaiyakul, N. Kaewnopparat, S. Ingkatawornwong, Properties of solid dispersions of piroxicam in polyvinylpyrrolidone, International Journal of Pharmaceutics 181 (2) (1999) 143–151.
[11] D. Douroumis, N. Bouropoulos, A. Fahr, Physicochemical characterization of solid dispersions of three antiepileptic drugs prepared by solvent evaporation method, Journal of Pharmacy and Pharmacology 59 (5) (2007) 645–653.
[12] D.J. Greenhalgh et al., Solubility parameters as predictors of miscibility in solid dispersions, Journal of Pharmaceutical Sciences 88 (11) (1999) 1182–1190.
[13] S. Okonogi, Improved dissolution of ofloxacin via solid dispersion, International Journal of Pharmaceutics 156 (2) (1997) 175–180.
[14] D.Q.M. Craig, The mechanisms of drug release from solid dispersions in water-soluble polymers, International Journal of Pharmaceutics 231 (2) (2002) 131–144.
[15] S. Mirza et al., Understanding processing-induced phase transformations in erythromycin – PEG 6000 solid dispersions, Journal of Pharmaceutical Sciences 95 (8) (2006) 1723–1732.
[16] D.I. Van Drooge, W.L.J. Hinrichs, H.W. Frijlink, Incorporation of lipophilic drugs in sugar glasses by lyophilization using a mixture of water and tertiary butyl alcohol as solvent, Journal of Pharmaceutical Sciences 93 (3) (2004) 713–725.
[17] N. Yuksel et al., Enhanced bioavailability of piroxicam using Gelucire 44/14 and Labrasol: in vitro and in vivo evaluation, European Journal of Pharmaceutics and Biopharmaceutics 56 (3) (2003) 453–459.
[18] C.P. Buckley, A.J. Kovacs, Melting behaviour of low molecular weight (ethylene-oxide) fractions I. Extended chain crystals, Progress in Colloid & Polymer Science 58 (1975) 44–52.
[19] C.P. Buckley, A.J. Kovacs, Melting behavior of low-molecular weight poly (ethylene-oxide) fractions.2. Folded chain crystals, Colloid and Polymer Science 254 (8) (1976) 695–715.
[20] S.Z.D. Cheng et al., Isothermal thickening and thinning processes in low-molecular-weight poly(ethylene oxide) fractions.1. From nonintegral-folding to integral-folding chain crystal transitions, Macromolecules 24 (13) (1991) 3937–3944.
[21] S.Z.D. Cheng et al., Nonintegral and integral folding crystal-growth in low-molecular mass poly(ethylene oxide) fractions.1. Isothermal lamellar thickening and thinning, Journal of Polymer Science Part B – Polymer Physics 29 (3) (1991) 287–297.
[22] H. Konno, L.S. Taylor, Influence of different polymers on the crystallization tendency of molecularly dispersed amorphous felodipine, Journal of Pharmaceutical Sciences 95 (12) (2006) 2692–2705.
[23] I. Weuts et al., Phase behaviour analysis of solid dispersions of loperamide and two structurally related compounds with the polymers PVP-K30 and PVP-VA64, European Journal of Pharmaceutical Sciences 22 (5) (2004) 375–385.
[24] F. Giordano, R. Bettini, C. Donini, A. Gazzangia, M.R. Caira, G.G.Z. Zhanf, D.J.W. Gramt, Physical properties of parabens and their mixtures: solubility in water, thermal behaviour and crystal structures, J. Pharm. Sci. 88 (1999) 1210–1216.
[25] Y. Cerenius et al., The crystallography beamline I711 at MAX II, Journal of Synchrotron Radiation 7 (2000) 203–208.
[26] A. Hammersley, The Fit2D home page, 2007 <http://www.esrf.eu/computing/scientific/FIT2D>.
[27] C.G. Vonk, G. Kortleve, X-ray small-angle scattering of bulk polyethylene.2. Analyses of scattering curve, Kolloid-Zeitschrift and Zeitschrift Fur Polymere 220 (1) (1967) 19–24.
[28] W. Ruland, Small-angle scattering of 2-phase systems – determination and significance of systematic deviations from Porods law, Journal of Applied Crystallography 4 (FEB1) (1971) 70–73.
[29] P. Debye, H.R. Anderson, H. Brumberger, Scattering by an inhomogeneous solid.2. The correlation function and its application, Journal of Applied Physics 28 (6) (1957) 679–683.
[30] P. Debye, A.M. Bueche, Scattering by an inhomogeneous solid, Journal of Applied Physics 20 (6) (1949) 518–525.
[31] D. Mahlin et al., Influence of polymer molecular weight on the solid-state structure of PEG/monoolein mixtures, Polymer 46 (26) (2005) 12210–12217.
[32] E. Karavas, E. Georgakis, M.P. Sigalas, K. Avgoustakis, D. Bikiaris, Investigation of the release mechanism of a sparingly water-soluble drug from solid dispersions in hydrophilic carriers based on physical state of drug, particle size distribution and drug–polymer interactions, European Journal of Pharmaceutics and Biopharmaceutics 66 (3) (2006) 334–347.